

## Articles

### Synthesis and Mixed Lineage Kinase Activity of Pyrrolocarbazole and Isoindolone Analogs of (+)K-252a

Robert L. Hudkins,\* Neil W. Johnson, Thelma S. Angeles, George W. Gessner, and John P. Mallamo

Cephalon, Inc., 145 Brandywine Parkway, West Chester, Pennsylvania 19380

Received October 24, 2005

Structural modification of the indolecarbazole natural product (+)K-252a identified structural requirements for MLK activity and a novel series of potent fused pyrrolocarbazole MLK1/3 inhibitors. The SAR revealed that the lactam regiochemistry, the shape of the heterocycle, and aryl rings B and F are important to MLK activity. Heteroatom and alkyl replacement of the N-12 and/or N-13 indole nitrogen atoms identified the nonplanar dihydronaphthyl[3,4-a]pyrrolo[3,4-c]carbazole-7-one (**8**) and corresponding 5,7-dione (**7**) as potent cell-permeable MLK1/3 family-selective leads with in vitro activity comparable to that of (+)K-252a and determined them to be 2- to 3-fold more potent than the aglycone natural product K-252c.

#### Introduction

Several lines of evidence indicate that neuronal apoptosis may be an important mechanism contributing to the progression of disability in Parkinson's disease (PD) and Alzheimer's disease (AD).<sup>1</sup> Although the few available therapies afford some degree of symptomatic relief, none prevents the progression of the disease or delays the pathological neuronal cell death associated with the disease. Activation of the c-jun-N-terminal kinase (JNK)<sup>a</sup> pathway, which is critical for naturally occurring neuronal cell death in development, has been shown to mediate apoptotic neuronal death in response to a variety of stimuli and may be important for the pathological cell death in neurodegenerative diseases.<sup>2</sup>

The JNKs (JNK1–3) are stress-activated protein kinases (SAPK) that belong to the mitogen-activated protein kinase (MAPK) superfamily and are the only kinases that phosphorylate the transcription factor cJun on Ser<sup>63</sup> and Ser<sup>73</sup>, an early initiating event in the cell death process.<sup>2,3</sup> The mixed-lineage kinases (MLK) are an important upstream activating component of the JNK signaling cascade and function to phosphorylate MAPK kinases MKK4 and MKK7 of the cascade.<sup>4</sup> The MLKs function as serine/threonine kinases, although their catalytic domains have features of both tyrosine and serine/threonine kinases. Overexpression of MLKs results in apoptotic cell death in PC12 cells and primary sympathetic neurons. Conversely, the expression of kinase-dead MLKs blocks apoptosis induced by trophic factor withdrawal.<sup>4,5</sup> Inhibitors of MLKs, and subsequently of JNK/cJun, have the potential not only for slowing the progression of the neurodegenerative diseases but also for improving the function of surviving neurons.

Our research has focused on the design of potent, selective inhibitors of MLKs for the treatment of AD and PD.<sup>6,7</sup> **1** (CEP-1347) was the first compound from this program to advance into clinical evaluation for Parkinson's disease.<sup>7a</sup> Preclinical pharmacology demonstrated that **1** promoted neuronal survival

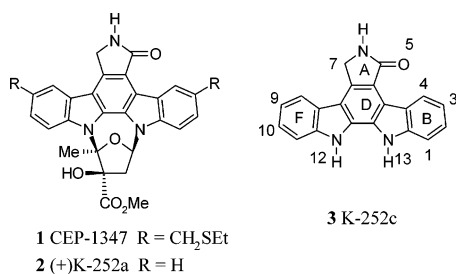
in several in vitro and in vivo models.<sup>7,8</sup> **1** attenuated the loss of tyrosine hydroxylase activity and dopamine transporter density after administration of 1-methyl-4-phenyl-tetrahydropyridine (MPTP) in mice<sup>9</sup> and reduced the development of neurologic dysfunction in monkeys treated with MPTP.<sup>7a,9</sup> Although **1** has no direct activity on JNK itself, the mechanism has been shown to be a result of JNK pathway inhibition via MLK.<sup>8</sup> **1** is a semisynthetic 3,9-bis-ethylthiomethyl derivative of the indolecarbazole natural product (+)K-252a (**2**).<sup>7a,10</sup> **2** is a nonselective ATP competitive inhibitor of numerous tyrosine and serine/threonine kinases. One of the drawbacks of **1** is the requirement for fermentation of the natural product starting material (originally fermented from the culture broth of *Nocardopsis* sp.).<sup>11</sup> An ensuing medicinal chemistry program was initiated to identify smaller, fully synthetic MLK1/3 inhibitors for PD. The initial objective was to define the minimum pharmacophore and structural features of **2** required for MLK activity in order to identify a starting core. Removal of the sugar from glycosylated **2** to produce the aglycone K-252c (**3**), a natural product produced by *Nocardopsis* strain K-290,<sup>12</sup> resulted in a molecule with MLK activity about 5-fold weaker than that of **2**, with IC<sub>50</sub> values of 138 nM for MLK1 and 49 nM for MLK3. Because the sugar moiety is not essential, our strategy was to conserve the lactam hydrogen bond donor/acceptor moiety, known to be a requirement for indolecarbazoles to bind at the conserved hinge region at the ATP site of kinases,<sup>13</sup> and modify the indolecarbazole ring system. We investigated the MLK structure–activity relationships (SAR) by making structural changes to the indolecarbazole core with heteroatom and alkyl replacements for the indole nitrogen. An important aspect of this work for interpreting the SAR was the establishment of the lactam carbonyl regiochemistry necessary for orientation of the scaffold at the hinge region for ATP competitive inhibitors.

#### Chemistry

Indenocarbazole imide **4** was prepared utilizing a Diels–Alder reaction with maleimide and 2-(2-indenyl)indole as described previously.<sup>14</sup> Lactam isomers **5** (7-oxo) and **6** (5-oxo) were prepared utilizing a regioselective Diels–Alder reaction with

\* Correspondence author: Tel: 610-738-6283. E-mail: rhudkins@cephalon.com.

<sup>a</sup> Abbreviations: MLK, mixed-lineage kinase; JNK, c-jun-N-terminal kinase; MKK, MAP kinase kinase; GST, glutathione S-transferase.



**Figure 1.** Structures of **1** (CEP-1347), **2** ((+)-K-252a), and **3** (K-252c).

2-(2-indenyl)indole and ethyl *cis*- $\beta$ -cyanoacrylate.<sup>14</sup> The individual tetrahydrocarbazole diastereomers were separated by recrystallization, aromatized to the cyano-ester carbazoles using DDQ, and then subjected to a reductive cyclization (RaNi, H<sub>2</sub>, DMF, MeOH) to produce the lactams. The regiochemistry and stereochemistry were assigned by <sup>1</sup>H NMR and 2D <sup>1</sup>H NMR experiments and confirmed by single-crystal X-ray crystallography.<sup>14</sup> Dihydronaphthyl imide **7** (Scheme 1) and lactam isomers **8** and **9** were produced in a similar manner starting with 2-(3,4-dihydronaphthyl)indole **10b** as the diene (Scheme 2). DDQ oxidation of **7** in dioxane produced **12**. Because of the difficulty in separating the cyano-ester tetrahydrocarbazole isomers (**13a**, **13b**; Scheme 2), the mixture was dehydrogenated to a mixture of carbazoles **14a** and **14b** and then underwent cyclization to produce a mixture of the lactam products. Regiosomers **8** and **9** were separated using silica gel column chromatography. Benzo[*b*]thieno- and benzo[*b*]furano[2,3-*a*]pyrrolo[3,4-*c*]carbazole imides **15** and **16** were prepared from Michael adducts 2-(2-benzo[*b*]thieno)- (**17**) and 2-(2-benzo[*b*]furano)-3-[3-(2,5-dioxo-1H-pyrrolidinyl)]indole (**18**) by a novel palladium(II)acetate/tetrachloro-1,4-benzoquinone oxidative A–E ring closure (Scheme 3).<sup>15</sup> Benzothiazophene and benzofuran imides **15** and **16** were then converted to the lactam regioisomers (**19**–**22**) using Clemmensen reduction conditions (zinc–mercury amalgam, EtOH, HCl) and separated by reverse-phase HPLC.<sup>15</sup> Biindene imide **23** was prepared from 2,2'-biindene<sup>16</sup> (**24**) and maleimide as shown in Scheme 4. DDQ dehydrogenation of **25** to **23** followed by a Clemmensen reduction produced lactam **26** in high yield (Scheme 4).<sup>17</sup> 2,2'-Biindene (**24**) was prepared by an improved method with palladium catalyzed coupling of 2-(tributylstannyl) indene (**27**) with 2-bromoindene.<sup>18</sup> Dibenzothiazophene imide **28** was prepared by the reaction of 2,2'-bibenzothiazophene **29** and diethyl acetylenedicarboxylate in a sealed tube at 190 °C (Scheme 5) to give diester **30**. Intermediate diester **30** was converted to the anhydride **31** with LiI/acetic anhydride in pyridine (Scheme 5). Anhydride **31** was treated with HMDS to produce imide **28**, followed by Clemmensen reduction conditions to produce lactam **32**. Using a similar procedure to prepare **28**, indeno-benzothiazophene imide **33** was prepared starting with 2-(2'-indenyl)benzothiazophene **34**. The lactam isomers **37** and **38** were separated using preparatory HPLC.

## Results and Discussion

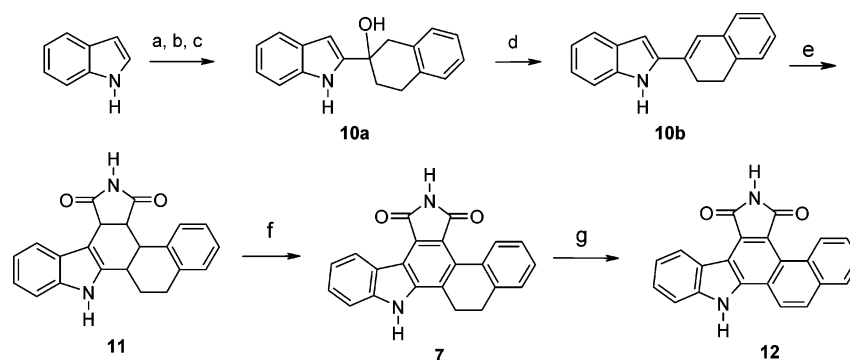
The pyrrolocarbazoles and isoindolones were tested for their MLK1 and MLK3 inhibitory activity against GST-tagged truncated kinase-active forms of the enzymes expressed from baculovirus constructs. The assays were established using myelin basic protein as a substrate via a radioactive multiscreen format. Shown in Table 1 is the MLK1/3 data for a set of lactam regioisomers, replacing the N-12 indole nitrogen with CH<sub>2</sub>, CH<sub>2</sub>-CH<sub>2</sub>, S, and O compared to compound **3** (K-252c) (MLK1 IC<sub>50</sub> = 138 nM, MLK3 IC<sub>50</sub> = 49 nM). Methylene analog **5** was

essentially equivalent, whereas ethylene bridge analog **8** displayed a 2- to 3-fold improvement in potency (MLK1 IC<sub>50</sub> = 46 nM, MLK3 IC<sub>50</sub> = 22 nM) over **3**. When the N-12 nitrogen was replaced with either sulfur (**19**) or oxygen (**21**), a 3–5-fold loss in activity for MLK3 was observed. **19** showed a 13-fold drop in MLK1 activity (IC<sub>50</sub> = 1.8  $\mu$ M). The data set for the lactam regioisomers is shown in Table 2. Methylene analog **6** was 2-fold more potent for MLK1 (IC<sub>50</sub> 138 nM) over **3** or its regiomere **5** and was also potent for MLK3 with an IC<sub>50</sub> value of 40 nM. The ethylene bridge analog **9**, contrary to its regiomere **8**, showed a significant loss in activity with IC<sub>50</sub> values of 1.1 and 0.7  $\mu$ M for MLK1 and MLK3, respectively. One explanation for the decrease in activity may be the lack of planarity between the D–B rings. The B–D-ring dihedral angle was 30° in C-ring expanded analog **9** due to the carbonyl-H4 crowding effect (Figure 2). The carbonyl deshielding effect on H-4 can be observed in <sup>1</sup>H NMR comparing **6** to **5** ( $\delta$  9.4 to  $\delta$  7.7).<sup>14</sup> Compounds **3**, **6**, and **20** were essentially planar, with the D–B-ring dihedral angle near 0°. The sulfur analog **20** also showed the reverse trend from its regiomere to more potent compounds, with IC<sub>50</sub> values of 111 and 26 nM for MLK1 and MLK3, respectively. The oxygen replacement **22** was not tolerated for either of the MLKs.

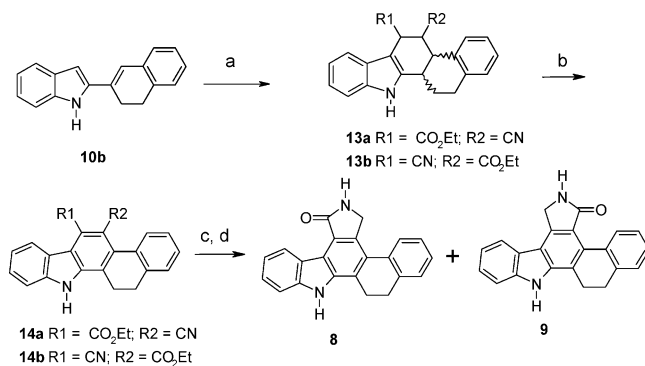
From this set of data, the most potent MLK profile was seen with the 7-oxo dihydronaphthyl analog **8** and with the indeno-carbazole (**6**) and benzothiazophene (**20**) regiomers. Shown in Table 3 is a set of analogs prepared to evaluate the effect of replacing both N-12 and N-13 simultaneously. In general, the replacement of both nitrogen atoms was not favorable. CH<sub>2</sub>–S isomers **37** and **38**, although weaker than **3**, were the top compounds from this set. Bis-CH<sub>2</sub> analog **26** showed 5-fold and 10-fold losses in activity, whereas sulfur analog **32** was inactive (IC<sub>50</sub> > 10  $\mu$ M). All attempts to prepare the bis-benzofuran counterpart were unsuccessful. The imide derivatives were also tested for MLK activity with the dihydronaphthyl analog **7** (X<sub>2</sub> = CH<sub>2</sub>CH<sub>2</sub>) displaying the most potent inhibitory profile with IC<sub>50</sub> values of 22 and 12 nM for MLK1 and MLK3, respectively (Table 4). Sulfur **15** was also tolerated, whereas imides **23**, **28**, and **33** lacking both N-12 and N-13 were weaker.

The emerging SAR indicated that the shape (derived from molecular modeling) and the bridging groups were important MLK activity. The order of activity for the pharmacophore represented by a planar B–C–D pyrrolocarbazole ring system was X<sub>1</sub> = CH<sub>2</sub>CH<sub>2</sub> > CH<sub>2</sub>  $\cong$  N > O > S when X<sub>2</sub> = N and X<sub>2</sub> = CH<sub>2</sub>  $\cong$  S  $\cong$  N > CH<sub>2</sub>CH<sub>2</sub> >> O when X<sub>1</sub> = N. To investigate this hypothesis further, we evaluated two pyrrolocarbazoles lacking the N-12 (**39**) or N-13 (**40**) indole nitrogen (Figure 3).<sup>19</sup> Analog **40** was inactive (IC<sub>50</sub> > 10  $\mu$ M) for both MLK1 and MLK3, whereas *des*-N-12 carbazole **39** retained weak activity with IC<sub>50</sub> values of 2.9  $\mu$ M for MLK1 and 1.2  $\mu$ M for MLK3. **39** also retained weak survival-promoting activity in the cholinergic spinal cord motoneuron assay, whereas **40** was inactive.<sup>19</sup> To evaluate the contribution of aryl rings B and F, *des*-aryl analogs **41** and **42** were tested and displayed IC<sub>50</sub> values > 1  $\mu$ M.<sup>20</sup> To further evaluate whether a linear or bent shape of the aryl rings was preferred, analogs **43** and **44**<sup>21</sup> were also tested and were inactive for MLK1 and MLK3.

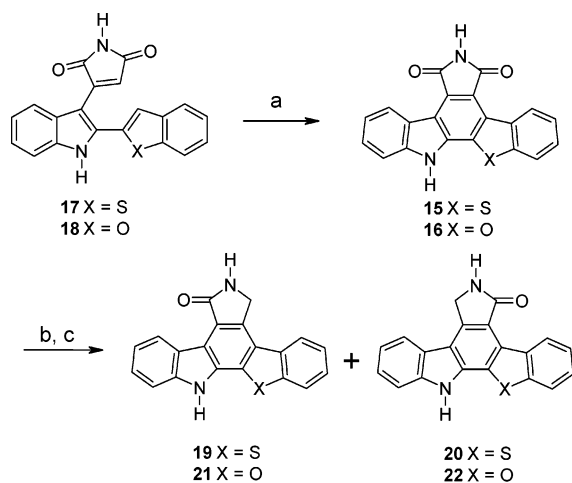
The inhibitory activity of scaffolds **5**, **6**, **7**, **8**, and **20** were profiled against related family members MLK2 and DLK and for selectivity against a set of serine/threonine and tyrosine kinases that represented targets for **2**, such as protein kinase-C<sup>10</sup> (PKC) (mixture of Ca<sup>2+</sup>-dependent isozymes  $\alpha$ ,  $\beta$ , and  $\gamma$ ), vascular endothelial growth factor receptor-2 (VEGF-R2),<sup>22</sup> and trkA.<sup>10,22,23</sup> (Table 3). Interestingly, the data in Table 5 show

Scheme 1<sup>a</sup>

<sup>a</sup> Reagents and conditions: (a) *n*-BuLi, THF, CO<sub>2</sub>(g), -78 °C. (b) *t*-BuLi, THF, -78 °C, 2-tetralones. (c) NH<sub>4</sub>Cl. (d) 1 N HCl, acetone. (e) Maleimide, 190 °C. (f) DDQ, C<sub>6</sub>H<sub>5</sub>CH<sub>3</sub>, 60–70 °C. (g) DDQ, dioxane, reflux.

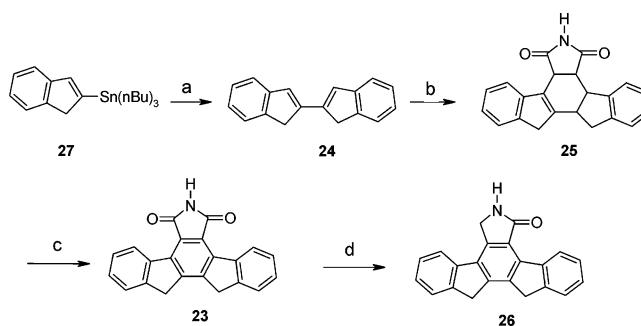
Scheme 2<sup>a</sup>

<sup>a</sup> Reagents and conditions: (a) *cis*-ethyl β-cyanoacrylate, 190 °C. (b) DDQ, C<sub>6</sub>H<sub>5</sub>CH<sub>3</sub>, 60–70 °C. (c) RaNi, H<sub>2</sub>, DMF, MeOH (d) Silica gel chromatography separation.

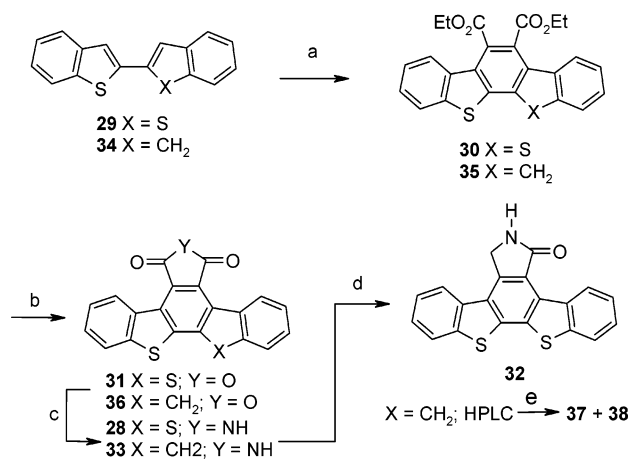
Scheme 3<sup>a</sup>

<sup>a</sup> Reagents and conditions: (a) Pd(OAc)<sub>2</sub>, C<sub>6</sub>Cl<sub>4</sub>O<sub>2</sub>, PhCl<sub>2</sub>, reflux. (b) ZnHg, HCl, EtOH, reflux. (c) Reverse-phase HPLC separation.

that the scaffolds displayed good selectivity for MLK1/3 within the family because they only weakly inhibited DLK, and only the 5-oxo indenocarbazole **6** inhibited MLK2 with an IC<sub>50</sub> value of 364 nM. The nonplanar dihydronaphthyl **8** showed activity for PKC (IC<sub>50</sub> = 205 nM) but weak activity for trkA and VEGF-R2. Planar indenocarbazoles **5** and **6** showed the opposite selectivity profile compared to that of **8**. Benzothiazophene **20** was a potent inhibitor of trkA with an IC<sub>50</sub> value of 85 nM and a weaker inhibitor of PKC and VEGF-R2. Compounds **5**, **6**, **7**, **8**, and **20** were screened further against PDGFRβ, EGFR,

Scheme 4<sup>a</sup>

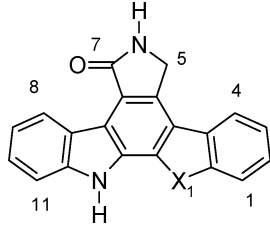
<sup>a</sup> Reagents and conditions: (a) 2-bromoindene, bis(triphenylphosphine) palladium(II) chloride, ethanol. (b) Maleimide, 190 °C. (c) DDQ, C<sub>6</sub>H<sub>5</sub>CH<sub>3</sub>, 60–70 °C. (d) ZnHg, HCl, EtOH, reflux.

Scheme 5<sup>a</sup>

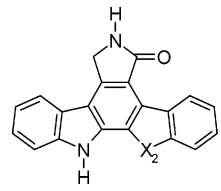
<sup>a</sup> Reagents and conditions: (a) diethyl acetylene dicarboxylate. (b) LiI, Ac<sub>2</sub>O, pyr. (c) HMDS, MeOH, DMF. (d) ZnHg, HCl, EtOH, reflux. (e) Reverse-phase HPLC separation.

FGFR1, CDK1, CDK2, p38α, TIE2, JNK1, and βIRK and displayed <30% inhibition at 1 μM.

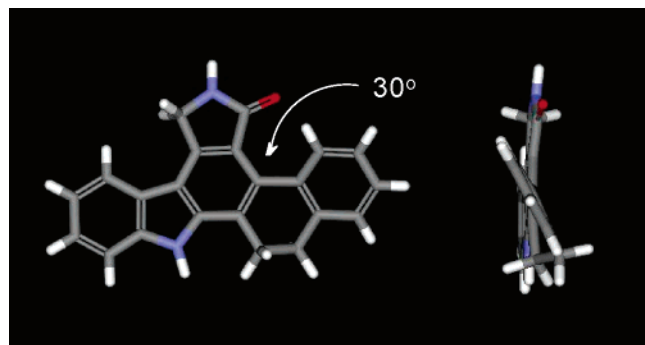
The more potent compounds **5**, **6**, **7**, **8**, and **20** were evaluated in an MLK1-cell-based assay for inhibition of MKK4 phosphorylation after a 1 h incubation. MLK1 was transfected into CHO cells with dominant negative MKK4 cDNA, and phospho-MKK4 was measured in an ELISA-based format as described previously.<sup>8</sup> **5**, **6**, and **20** were weak to inactive for MLK1 cell activity tested up to 1 μM concentration, signifying poor cell permeability. However, dihydronaphthyl imide **7** (MLK1 enzyme IC<sub>50</sub> = 22 nM) and 7-oxo lactam **8** (MLK1 enzyme IC<sub>50</sub> = 46 nM) displayed good MLK1 cell activity profiles with IC<sub>50</sub> values of 90 and 274 nM, respectively (Table 6). **7** and **8** display

**Table 1.** MLK1 and MLK3 Activity of N-12-Replaced ( $X_1$ ) Pyrrolo[3,4-*c*]carbazole Analogs


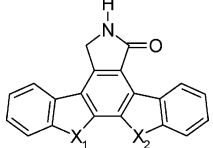
entry	$X_1$	MLK1 <sup>a</sup>	MLK3 <sup>a</sup>
<b>3</b>	NH	138	49
<b>5</b>	CH <sub>2</sub>	167	87
<b>8</b>	CH <sub>2</sub> CH <sub>2</sub>	46	22
<b>19</b>	S	1795	171
<b>21</b>	O	308	270

<sup>a</sup> IC<sub>50</sub> values are reported in nanomolar.**Table 2.** MLK1 and MLK3 Activity of N-13-Replaced ( $X_2$ ) Pyrrolo[3,4-*c*]carbazole Analogs


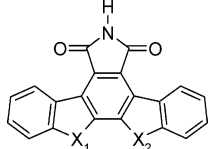
entry	$X_2$	MLK1 <sup>a</sup>	MLK3 <sup>a</sup>
<b>3</b>	NH	138	49
<b>6</b>	CH <sub>2</sub>	69	40
<b>9</b>	CH <sub>2</sub> CH <sub>2</sub>	1106	724
<b>20</b>	S	111	26
<b>22</b>	O	> 10000	1106

<sup>a</sup> IC<sub>50</sub> values are reported in nanomolar.**Figure 2.** MOPAC-minimized structure and shape of **9**.

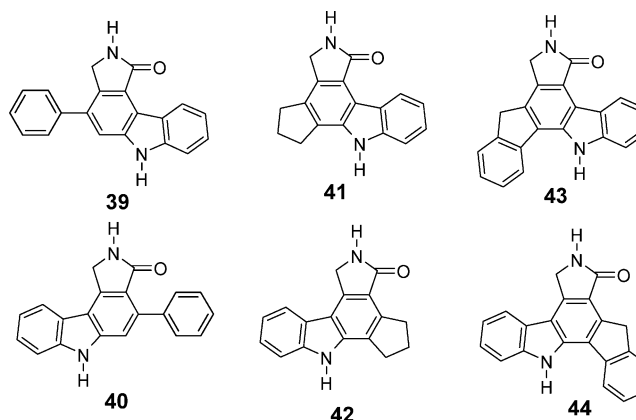
approximately a 4-fold shift from the cell-free-isolated MLK1 enzyme activity. The cell permeability of the dihydronaphthyl core compared favorably with the cell activity of the optimized semisynthetic **2**-derived clinical compound **1** (MLK1 enzyme IC<sub>50</sub> = 38 nM; MLK1 cell IC<sub>50</sub> = 72 nM).<sup>6</sup> The best compounds were further evaluated for functional survival promoting activity as measured by the ability to enhance ChAT activity in embryonic rat spinal cord cultures.<sup>24</sup> ChAT catalyzes the synthesis of the neurotransmitter acetylcholine and is considered to be a specific biochemical marker for functional cholinergic neurons. In the spinal cord, motor neurons are cholinergic and express ChAT.<sup>25</sup> ChAT activity has been used extensively to study the effects of **2**, indolocarbazole analogs, and neurotrophins on the survival and/or function of cholinergic neurons.<sup>6,7a,10,19,24,26</sup> In spinal cord cultures (E14–E19), a significant number of cholinergic neurons would be expected to die in the absence of a motor neuron survival factor, and a continual

**Table 3.** MLK1 and MLK3 Activity of Lactam N-12 and N-13 Replacement Analogs


entry	$X_1$	$X_2$	MLK1 <sup>a</sup>	MLK3 <sup>a</sup>
<b>3</b>	NH	NH	138	49
<b>26</b>	CH <sub>2</sub>	CH <sub>2</sub>	1415	277
<b>32</b>	S	S	> 10 000	> 10 000
<b>37</b>	S	CH <sub>2</sub>	482	157
<b>38</b>	CH <sub>2</sub>	S	615	110

<sup>a</sup> IC<sub>50</sub> values are reported in nanomolar.**Table 4.** MLK1 and MLK3 Activity of Imide Analogs


entry	$X_1$	$X_2$	MLK1 <sup>a</sup>	MLK3 <sup>a</sup>
<b>3</b>	NH	NH	> 300	> 300
<b>4</b>	NH	CH <sub>2</sub>	> 300	> 300
<b>7</b>	NH	CH <sub>2</sub> CH <sub>2</sub>	22	12
<b>12</b>	NH	CH=CH	~300	~300
<b>15</b>	NH	S	68	58
<b>16</b>	NH	O	> 300	> 300
<b>23</b>	CH <sub>2</sub>	CH <sub>2</sub>	> 300	> 300
<b>28</b>	S	S	> 300	> 300
<b>33</b>	S	CH <sub>2</sub>	> 300	> 300

<sup>a</sup> IC<sub>50</sub> values are reported in nanomolar.**Figure 3.** Structures of pyrrolo[3,4-*c*]carbazole modifications.

decline in ChAT activity is observed with increasing culture time.<sup>24a</sup> In this assay K-252a was used as an internal control for direct comparison of the functional activity in the ChAT assay experiments. K-252a was ineffective in the spinal ChAT assay at concentrations of less than 100 nM and showed a maximum enhancement of ChAT activity of 186 ± 3% above basal levels (100%) at 300 nM. Above 300 nM, K-252a showed a decrease in ChAT activity due to toxicity.<sup>16</sup> The analogs were evaluated for ChAT activity in the spinal cord cultures at 300 nM after 2 days in culture for maximum efficacy. The experimental data shown in Table 6 represents the mean ± the standard deviation from the three independent experiments. Analogs **5**, **6**, and **20** showed a maximum enhancement of ChAT activity at 155, 152, and 138%, respectively. The dihydronaph-

**Table 5.** MLK and Kinase Selectivity Profile of Selected Analogs

entry	X <sub>1</sub>	MLK1 <sup>a</sup>	MLK3 <sup>a</sup>	MLK2 <sup>a</sup>	DLK <sup>a</sup>	PKC <sup>a</sup>	TrkA <sup>a</sup>	VEGF-R2 <sup>a</sup>
<b>2</b>	<b>2(+)</b> K-252a	22	13	45	360	250	13	43
<b>5</b>	CH <sub>2</sub>	167	87	2664	>1000	>1000	155	414
<b>6</b>	CH <sub>2</sub>	69	40	364	>1000	1196	162	110
<b>7</b>	CH <sub>2</sub> CH <sub>2</sub>	22	12	339	487	83	>1000	>300
<b>8</b>	CH <sub>2</sub> CH <sub>2</sub>	46	22	3447	>1000	205	>1000	>300
<b>20</b>	S	111	26	2088	>1000	>1000	88	>300

<sup>a</sup> IC<sub>50</sub> values are reported in nanomolar.

**Table 6.** In Vitro MLK1 Cell and Functional Activity

entry	MLK1 <sup>a</sup>	MLK1 cell activity <sup>b</sup>	spinal cord ChAT <sup>c</sup>
<b>2</b>	22	NT	181 ± 3
<b>5</b>	167	22%	166 ± 8
<b>6</b>	69	19%	152 ± 14
<b>7</b>	22	90	178 ± 2
<b>8</b>	46	274	171 ± 15
<b>16</b>	>300	NT	inactive
<b>20</b>	111	3%	138 ± 1
<b>22</b>	>10000	NT	inactive
<b>23</b>	>300	NT	inactive
<b>32</b>	>10000	NT	inactive

<sup>a</sup> IC<sub>50</sub> values are reported in nanometers. <sup>b</sup> IC<sub>50</sub> values are reported in nanomolar or percent inhibition at 1 μM. NT = not tested. <sup>c</sup> Percent of control at 300 nM.

thyl derivatives **7** and **8** promoted the survival of spinal cord motor neurons and enhanced ChAT activity by 178 and 171% at 300 nM. Weak to inactive MLK inhibitors **16**, **21**, **22**, **23**, and **32** were also inactive in this assay at 300 nM concentrations.

In conclusion, this work identified a novel series of potent fused pyrrolocarbazole MLK1/3 inhibitors by the modification of indolecarbazole natural product **2**. The SAR revealed that the lactam regiochemistry, the shape of the heterocycle, and aryl rings B and F are important MLK activity. Heteroatom and alkyl replacement of the N-12 and/or N-13 indole nitrogen atoms identified the nonplanar dihydronaphthyl[3,4-*a*]pyrrolo[3,4-*c*]carbazole-7-one (**8**) and corresponding 5,7-dione (**7**) as potent MLK1/3 family selective leads with in vitro activity comparable to that of **2** and determined them to be 2- to 3-fold more potent than the aglycone natural product K-252c. The dihydronaphthyl ring system demonstrates good cell potency and selectivity against a panel of serine/threonine and tyrosine kinases representing a novel scaffold for further optimization. Lead optimization and MLK1 crystallography on the dihydronaphthyl scaffold leading to the progression of development compounds will be reported in due course.

## Experimental Section

**Chemistry.** All reagents and anhydrous solvents were obtained from commercial sources and used as received. <sup>1</sup>H and <sup>13</sup>C NMR were obtained at 300 or 400 MHz in the solvent indicated with tetramethylsilane as an internal standard. Coupling constants (*J*) are in Hertz (Hz). Analytical HPLC was run using a Zorbax RX-C8 5 × 150 mm<sup>2</sup> column eluted with a mixture of acetonitrile and water containing 0.1% trifluoroacetic acid with a gradient of 10–100%. Column chromatography was performed on silica gel 60 (230–400 mesh).

**2-2-(2-Hydroxy-1,2,3,4-tetrahydronaphthyl)indole (10a).** *n*-BuLi (85.3 mmol, 34 mL of 2.5 M sol in hexanes) was added dropwise to a solution of indole (10.0 g, 85.3 mmol) in dry THF (500 mL) at –78 °C under a nitrogen atmosphere for 15 min. The solution was stirred for 0.5 h, after which CO<sub>2</sub>(g) was passed through for 10 min. The solution was warmed to room temperature, and then excess CO<sub>2</sub>(g) was removed at reduced pressure. The solution was cooled to –78 °C, and a solution of *t*-BuLi (85.3 mmol, 50 mL of a 1.7 M solution in hexanes) was then added

dropwise. The resulting yellow solution was allowed to stir for 2 h at –78 °C and then 2-tetralone (13.7 g, 12.9 mL, 93.7 mmol) in THF (30 mL) was added dropwise, and the mixture was stirred for 1 h. The reaction was quenched by the addition of water (5 mL), poured into a saturated NH<sub>4</sub>Cl solution (250 mL), and extracted with ether (2 × 200 mL). The Et<sub>2</sub>O layer was washed with 100 mL of a saturated NH<sub>4</sub>Cl solution followed by drying (MgSO<sub>4</sub>) and concentration to give an oil. Recrystallization from MeOH gave 10 g (45%) of **10a** as a white solid: mp 191–192 °C. <sup>1</sup>H NMR (DMSO-*d*<sub>6</sub>) δ: 2.08–2.16 (m, 2H), 2.57–2.63 (m, 1H), 2.95–3.02 (m, 1H), 3.03 (d, *J* = 16.7 Hz, 1H), 3.28 (d, *J* = 16.8 Hz, 1H), 5.31 (s, 1H), 6.15 (s, 1H), 6.88 (t, *J* = 7.3 Hz, 1H), 6.98 (t, *J* = 7.7 Hz, 1H), 7.04–7.08 (m, 2H), 7.31 (d, *J* = 7.9 Hz, 1H), 7.38 (d, *J* = 7.7 Hz, 1H), 10.98 (s, 1H). MS *m/z*: 264 (M + 1). <sup>13</sup>C NMR (DMSO-*d*<sub>6</sub>) δ: 26.4, 34.8, 42.5, 68.5, 97.2, 111.6, 119.0, 120.1, 120.9, 125.9, 126.0, 128.1, 128.8, 129.5, 135.4, 135.9, 136.5, 146.8. Anal. Calcd for C<sub>18</sub>H<sub>17</sub>NO (C, H, N).

**2-(3,4-Dihydronaphth-2-yl)-1H-indole (10b).** A stirred solution of **10a** (5.0 g, 19.0 mmol) in acetone (150 mL) was added to 2 N HCl (5 mL) at room temperature. The solution was stirred for 1 h, and then water (ca. 25 mL) was added. The precipitate was collected by filtration, washed well with water, and dried to give 4.5 g (97%) of **10b**: mp 179–180 °C. (MeOH). <sup>1</sup>H NMR (DMSO-*d*<sub>6</sub>) δ: 2.71 (t, *J* = 7.7 Hz, 2H), 2.89 (t, *J* = 8.4 Hz, 2H), 6.67 (s, 1H), 6.98 (t, *J* = 7.1 Hz, 1H), 7.09–7.23 (m, 6H), 7.38 (d, *J* = 8.0 Hz, 1H), 7.50 (d, *J* = 7.8 Hz, 1H), 11.37 (s, 1H). <sup>13</sup>C NMR (DMSO-*d*<sub>6</sub>) δ: 24.7, 27.8, 101.16, 111.4, 119.6, 120.6, 121.7, 122.6, 126.7, 127.2, 127.3, 127.8, 128.7, 130.7, 134.6, 135.1, 137.9, 138.6. MS(ES<sup>+</sup>) *m/z*: 246 (M<sup>+</sup>). Anal. Calcd for C<sub>18</sub>H<sub>15</sub>N (C, H, N).

**4c,7a,7b,12,13,13a-Hexahydro-6H,14H-naphthyl[3,4-*a*]pyrrolo[3,4-*c*]carbazole-5,7-(5H,7H)dione (11).** A stirred mixture of **10b** (500 mg, 2.0 mmol) and maleimide (300 mg, 3.1 mmol) in a sealed reaction vial was held at 180–190 °C in an oil bath for 0.5 h. After cooling to ambient temperature, MeOH (5 mL) was added. The product was precipitated, triturated, and collected to give 610 mg (89%) of **11** as a mixture of two diastereomers. The product was used directly in the next step: mp 256–258 °C. <sup>1</sup>H NMR (DMSO-*d*<sub>6</sub>) δ: 1.60–1.77 (m, 0.5 H) 2.09–2.13 (m, 0.5 H), 2.87–2.92 (m, 2H), 3.13–3.20 (m, 2.5 H), 3.40 (m, 1H), 3.88–3.92 (m, 1H), 4.07–4.10 (m, 0.5 H), 4.22 (d, *J* = 7.7 Hz, 1H), 6.94–7.14 (m, 5H), 7.25–7.34 (m, 2H), 7.8 (m, 1H), 10.88 (s, 1H), 11.09 (s, 1H). MS *m/z*: 343 (M + 1).

**12,13-Dihydro-6H,14H-naphthyl[3,4-*a*]pyrrolo[3,4-*c*]carbazole-5,7-(5H,7H)dione (7).** Solid 2,3-dichloro-5,6-dicyano-1,4-benzoquinone (930 mg, 4.1 mmol) was added in one portion to a solution of **11** (400 mg, 1.2 mmol) in toluene (50 mL). The solution was maintained at 60–65 °C for 6 h. After cooling in an ice bath, the solid was collected by filtration, suspended in MeOH (20 mL), stirred for 0.5 h, and collected to give 320 mg (79%) of **7**: mp 258–260 °C. <sup>1</sup>H NMR (DMSO-*d*<sub>6</sub>) δ: 2.87 (t, *J* = 4.9 Hz, 2H), 3.07 (t, *J* = 6.8 Hz, 2H), 7.23–7.34 (m, 4H), 7.48–7.57 (m, 2H), 8.09–8.92 (m, 1H), 8.90 (d, *J* = 8.0 Hz, 1H), 11.05 (s, 1H), 11.95 (s, 1H). <sup>13</sup>C NMR (DMSO-*d*<sub>6</sub>) δ: 24.6, 28.3, 112.0, 117.8, 119.7, 120.7, 121.2, 125.7, 126.2, 127.6, 127.7, 127.8, 128.6, 128.7, 129.9, 131.0, 131.2, 138.6, 142.3, 142.6, 170.4, 170.8. MS(FAB) *m/z*: 338 (M<sup>+</sup>). Anal. Calcd for C<sub>22</sub>H<sub>14</sub>N<sub>2</sub>O<sub>2</sub> (C, H, N).

**6H,14H-Naphthyl[3,4-*a*]pyrrolo[3,4-*c*]carbazole-5,7-(5H,7H)-dione (12).** Solid 2,3-dichloro-5,6-dicyano-1,4-benzoquinone (465 mg, 2.1 mmol) was added in one portion to a solution of **7** (200 mg, 0.59 mmol) in dry dioxane (30 mL). The mixture was stirred

at reflux for 12 h, and then cooled to room temperature and filtered. The solvent was concentrated at reduced pressure. The solid residue was held at reflux in MeOH (25 mL), cooled to room temperature, and collected to yield 120 mg (61%) of **12**. Recrystallization from THF–MeOH gave **12** as a brown solid: mp > 330 °C. <sup>1</sup>H NMR (DMSO-*d*<sub>6</sub>) δ: 7.4 (t, 1H), 7.6 (t, 1H); 7.7–7.8 (m, 3H), 8.1 (m, 1H), 8.2 (d, 1H), 8.6 (d, 1H), 9.1 (d, 1H), 10.0 (m, 1H), 11.2 (s, 1H), 12.9 (s, 1H). MS(FAB) *m/z*: 336 (M<sup>+</sup>). Anal. Calcd for C<sub>22</sub>H<sub>12</sub>N<sub>2</sub>O<sub>2</sub>·0.1 H<sub>2</sub>O (C, H, N).

**3-Cyano-4-ethoxycarbonyl-1,2,3,4-tetrahydro-1,2-dihydronaphthyl[3,4-*a*]-9H-carbazole (13a) and 4-Cyano-3-ethoxycarbonyl-1,2,3,4-tetrahydro-1,2-didronaphthyl[3,4-*a*]-9H-carbazole (13b).** A mixture of **10** (1.0 g, 4.1 mmol) and ethyl *cis*-β-cyanoacrylate (5.0 g, 40 mmol) was heated in a sealed reaction flask and held at 180 °C with stirring for 1 h. The mixture was cooled to room temperature and transferred to a round-bottomed flask, and excess cyanoacrylate was removed by Kugelrohr distillation (oven temperature 80–85 °C, 0.5 mm). MeOH (25 mL) was added to the residue, and the product was triturated to give 700 mg (46%) of a white solid. The <sup>1</sup>H NMR showed approximately a 2:1 mixture of **13a/13b**. <sup>1</sup>H NMR (DMSO-*d*<sub>6</sub>) δ: 1.25 (t, 3H), 3.1–3.35 (m, 3H), 3.8 (s, m, 4H), 3.9 (m, 1H), 4.3–4.55 (m, 2H), 4.6 (d, 1H), 6.7 (d, 1H), 6.95 (s, 1H), 7.05–7.25 (m, 5H), 11.1 (s, 1H). The mixture was used directly in the next step.

**3-Cyano-4-ethoxycarbonyl-1,2-di-hydronaphthyl[3,4-*a*]-9H-carbazole (14a) and 4-Cyano-3-ethoxycarbonyl-1,2-di-hydronaphthyl[3,4-*a*]-9H-carbazole (14b).** 2,3-Dichloro-5,6-dicyano-1,4-benzoquinone (900 mg, 4.0 mmol) was added in one portion to a stirred solution of a 2:1 mixture of **13a/13b** (590 mg, 1.6 mmol) in dry toluene (50 mL). The solution was stirred at 65–70 °C for 6 h and cooled to room temperature, and the precipitate was removed by filtration and washed with toluene (10 mL). The toluene solution was concentrated at reduced pressure to yield a crude solid. Purification by column chromatography (silica gel, EtOAc/hexanes 2:1) gave 510 mg (87%) of an off-white solid with a composition of 2:1**14a/14b**. <sup>1</sup>H NMR (DMSO-*d*<sub>6</sub>) δ: 1.15 and 1.4 (t, 3H), 2.9 and 3.1–3.2 (q, 2H), 4.35 and 4.6 (q, 2H), 7.2–7.7 (m, 4H), 7.9 (d, 0.5H), 8.2 (d, 0.5H), 8.4 (d, 1H), 12.2 (d, 1H). The mixture was used directly in the next step.

**12,13-Dihydro-5H,6H,14H-naphthyl[3,4-*a*]pyrrolo[3,4-*c*]carbazole-7(7H)one (8) and 12,13-dihydro-6H,7H,14H-naphthyl[3,4-*a*]pyrrolo[3,4-*c*]carbazole-5(5H)one (9).** The mixture of isomers **14a/14b** from the preceding step (300 mg, 0.81 mmol) was added to a Raney nickel catalyst (ca. 1 g, wet form) in 100 mL of 3:1 DMF/MeOH and hydrogenated at 35 psi on a Parr apparatus for 16 h. The solution was diluted with DMF (50 mL), filtered through celite, and concentrated at reduced pressure to give 210 mg (80%) of a mixture of lactam isomers. The compounds were separated by silica gel column chromatography (2:1 EtOAc/hexanes). The fractions containing products were pooled and concentrated at reduced pressure. The products were recrystallized from MeOH–ether and dried (100 °C, 0.5 mm, 12 h) to give white solids. **8**: *R*<sub>f</sub> = 0.3; mp > 300 °C. <sup>1</sup>H NMR (DMSO-*d*<sub>6</sub>) δ: 2.91 (t, *J* = 5.2 Hz, 2H), 3.20 (t, *J* = 6 Hz, 2H), 4.87 (s, 2H), 7.19 (t, *J* = 7.3 Hz, 1H), 7.30–7.47 (m, 4H), 7.55 (d, *J* = 8.1 Hz, 1H), 7.83 (d, *J* = 7.7 Hz, 1H), 8.74 (s, 1H), 9.16 (d, *J* = 7.9 Hz, 1H), 11.57 (s, 1H). <sup>13</sup>C NMR (DMSO-*d*<sub>6</sub>) δ: 24.2, 28.6, 47.8, 111.3, 118.0, 119.3, 122.3, 124.9, 126.3, 126.5, 126.7, 126.8, 126.8, 127.5, 127.7, 128.7, 133.6, 134.1, 138.4, 138.6, 141.4, 171.8. MS(FAB) *m/z*: 325 (M + 1). Anal. Calcd for C<sub>22</sub>H<sub>16</sub>N<sub>2</sub>O·0.1 H<sub>2</sub>O (C, H, N). **9**: *R*<sub>f</sub> = 0.25, mp > 300 °C. <sup>1</sup>H NMR (DMSO-*d*<sub>6</sub>) δ: 2.87 (t, *J* = 5.6 Hz, 2H), 3.05 (t, *J* = 7.2 Hz, 2H), 4.82 (s, 2H), 7.22–7.34 (m, 4H), 7.47 (t, *J* = 7.8 Hz, 1H), 7.60 (d, *J* = 8.1 Hz, 1H), 8.00 (d, *J* = 7.7 Hz, 1H), 8.21 (m, 1H), 8.43 (s, 1H), 11.70 (s, 1H). <sup>13</sup>C NMR (DMSO-*d*<sub>6</sub>) δ: 24.2, 28.9, 44.1, 111.9, 116.2, 119.3, 120.2, 122.2, 122.3, 125.9, 126.4, 127.3, 127.5, 130.9, 131.9, 132.3, 138.0, 140.0, 140.3, 141.1, 171.7. MS(FAB) *m/z*: 325 (M + 1). Anal. Calcd for C<sub>22</sub>H<sub>16</sub>N<sub>2</sub>O·0.25 H<sub>2</sub>O: (C, H, N).

**2-(Tributylstannyl) Indene (27).** To a round-bottomed flask containing 2-bromoindene (1.64 g, 8.4 mmol) in NEt<sub>3</sub> (75 mL) was added palladium(II) acetate (304 mg, 11.4 mmol), tetrakis(tri-

phenylphosphine) palladium(0), (775 mg, 0.7 mmol), and hexabutyl-ditin (6.4 mL, 12.7 mmol). The reaction was held at reflux and monitored by TLC (silica gel, 1:5 EtOAc/hexanes). After 1 h, the starting material was consumed. The reaction was allowed to cool to room temperature, was diluted with CH<sub>2</sub>Cl<sub>2</sub>, and was filtered through celite. The solvent was removed at reduced pressure, and the compound was purified through a silica gel column (5% EtOAc–hexanes) to give 4.7 g of 2-tributylstannyl indene as a clear oil (containing traces of hexabutyl-ditin). The compound was used as is for the next step. <sup>1</sup>H NMR (CDCl<sub>3</sub>) δ: 0.9 (m, 15H), 1.2 (m, 6H), 1.6 (m, 6H), 3.5(s, 2H), 7.10 (s, 1H), 7.5–7.2 (m, 4H).

**2,2'-Biindene (24).** To a 100 mL round-bottomed flask, fitted with a reflux condenser, was added 2-bromoindene (1.2 g, 6.3 mmol), **27** (3.4 g, 8.4 mmol), and ethanol (70 mL). To this mixture was added bis(triphenylphosphine) palladium(II) chloride (442 mg, 0.63 mmol). The reaction was stirred at reflux for 16 h. The reaction was allowed to cool to room temperature, diluted with diethyl ether (50 mL), and then filtered through a pad of alumina. The solvent was concentrated at reduced pressure, and the product was recrystallized from toluene to give 870 mg (60%) of **24**: mp 238 °C (lit. mp = 238 °C<sup>16</sup>). <sup>1</sup>H NMR (CDCl<sub>3</sub>) δ: 3.73 (s, 4H), 6.93 (s, 2H), 7.30 (m, 8H). MS *m/z*: 231 (M + 1).

**1a,3a,4,7-Tetrahydroindeny[2,3-*c*]indeny[2,3-*e*]isoindol-1,3-dione (25).** To a sealable borosilicate reaction tube was added **24** (98 mg, 0.4 mmol), maleimide (43 mg, 0.44 mmol), BHT (5 mg), and CH<sub>2</sub>Cl<sub>2</sub> (1 mL). The tube was sealed, and the reaction was held at 130 °C in an oil bath for 24 h. The reaction was allowed to cool to room temperature, and the solvent was concentrated at reduced pressure. The crude solid was purified via column chromatography (silica gel, 10–75% EtOAc–hexane) to give 50 mg (38%) of **25** as a white solid: mp 244–247 °C. <sup>1</sup>H NMR (CDCl<sub>3</sub>) δ: 3.68 (s, 4H), 3.80 (m, 2H), 4.00 (bs, 2H), 7.24 (m, 7H), 7.53 (d, *J* = 7 Hz, 2H). MS *m/z*: 328 (M + 1).

**1H-Indeny[2,3-*c*]-1H-indeny[2,3-*e*]isoindol-1,3-dione (23).** A mixture of **25** (50 mg, 0.15 mmol) in toluene (4 mL) was added to solid 2,3-dichloro-5,6-dicyano-1,4-benzoquinone (79 mg, 0.35 mmol) in one portion. The reaction was heated under nitrogen at 65–70 °C for 4 h. The solution was cooled in an ice bath, and the solid material was collected by filtration. The crude precipitate was washed with cold methanol, leaving a pale-yellow solid (28 mg, 63%): mp 244–247 °C. <sup>1</sup>H NMR (CDCl<sub>3</sub>) δ: 9.17 (d, *J* = 4 Hz, 2H), 7.55 (m, 7H), 4.15 (s, 4H); MS *m/z*: 324 (M + 1). Anal. Calc. for C<sub>22</sub>H<sub>13</sub>NO<sub>2</sub> (C, H, N).

**1H-Indeny[2,3-*c*]-1H-indeny[2,3-*e*]-3H-isoindol-1-one (26).** A zinc amalgam was prepared by suspending zinc dust (122 mg, 1.9 mmol) in 1 mL of water and adding HgCl<sub>2</sub> (35 mg, 0.08 mmol) followed by 4 drops of concentrated HCl. This mixture was stirred for 10 min, and the aqueous layer was decanted off. The amalgam was washed with water and then washed repeatedly with EtOH. The above zinc amalgam was suspended in 5 mL of EtOH, and **23** (10 mg, 0.03 mmol) was added. A few drops of concentrated HCl were added, and the reaction was held at reflux for 3 h. The yellow color disappeared during the first hour of heating. The reaction was allowed to cool to room temperature, and the solution was concentrated at reduced pressure. The residue was dissolved in 10 mL of THF–EtOAc (1:1) and washed with saturated NaHCO<sub>3</sub> and NaCl solutions and then dried (MgSO<sub>4</sub>). The drying agent was removed by filtration, and the solvent was concentrated at reduced pressure to give 8 mg (88%) of lactam **26** as a white solid: mp 256 °C. <sup>1</sup>H NMR (CDCl<sub>3</sub>) δ: 9.20 (d, *J* = 8 Hz, 1H), 7.50 (m, 6H), 6.24 (s, 1H), 4.83 (s, 2H), 4.05 (s, 2H), 3.95 (s, 2H); MS *m/z*: 310 (M + 1). Anal. Calc. for C<sub>22</sub>H<sub>13</sub>NO (C, H, N).

**2,2'-Bibenzothiaphene (29).** To a two-necked round-bottomed flask fitted with a reflux condenser was added 2-bromobenzothiaphene (3.3 g, 15.6 mmol), 2-(tri-*n*-butyltin)benzothiaphene (7.3 g, 17 mmol), and toluene (40 mL). To this mixture was added tetrakis(triphenylphosphine) palladium(0) (360 mg, 0.3 mmol) and BHT (5 mg). The reaction was held at reflux for 16 h. After cooling to room temperature, the solvent was removed under vacuum, and the reaction was dissolved in DMF and filtered through celite. The solvent was removed under vacuum, and the solid was triturated

with hexanes to give 3.58 g (13.4 mmol, 85% yield) of 2,2'-bibenzothiophene **29** as a silver-black solid: mp 260–262 °C. <sup>1</sup>H NMR (DMSO-*d*<sub>6</sub>) δ: 7.98 (m, 2H), 7.62 (s, 1H), 7.36 (m, 2H), 7.25 (s, 1H).

**3,4-Carboethoxybenzothienyl[1,2-*a*]dibenzothiophene (30).** In a sealable glass tube was placed **29** (1.02 g, 3.8 mmol), diethyl acetylenedicarboxylate (3.1 mL, 19 mmol), and BHT (5 mg). The reaction vessel was sealed under N<sub>2</sub> and held at 190 °C. The reaction was allowed to proceed for 24 h. After allowing the reaction vessel to cool, the contents were transferred to a round-bottomed flask using CHCl<sub>3</sub>, and the solvent was removed under vacuum. The solid was taken up in diethyl ether and filtered, giving 468 mg (1.07 mmol, 28%) of 3,4-carboethoxybenzothienyl[1,2-*a*]dibenzothiophene as a pale-yellow solid. A second crop afforded 280 mg of material for a total yield of 45%: mp 206–207 °C. <sup>1</sup>H NMR (DMSO-*d*<sub>6</sub>) δ: 8.27 (d, *J* = 7.4 Hz, 2H), 8.05 (d, *J* = 7.9 Hz, 2H), 7.65 (m, 4H), 4.57 (q, *J* = 7.1 Hz, 4H), 1.38 (t, *J* = 7.1 Hz, 6H).

**Benzothieno[2,3-*c*]benzothieno[2,3-*e*]isoindol-1,3-dione (28).** (a) A round-bottomed flask was charged with **30** (500 mg, 1.15 mmol) and DMF (50 mL). To this mixture was added sodium cyanide (124 mg, 2.5 mmol) and solid lithium iodide trihydrate (476 mg, 2.5 mmol). The reaction was held at 150 °C and followed by TLC. Additional NaCN/LiI was added as time progressed. A total of 4 equiv each of NaCN and LiI was added over a reaction time of 36 h, at which time the starting material was totally consumed. The reaction mixture was cooled to room temperature and poured over cold (0 °C) aqueous HCl. The mixture was filtered and washed with water. The resultant solid was dried under vacuum. The above crude solid was then placed in a round-bottomed flask, and 50 mL of acetic anhydride was added. The reaction mixture was then held at reflux. After 4 h at reflux, the reaction was complete by TLC (new spot at *R*<sub>f</sub> 0.65 in 1:1 EtOAc/hexanes). The solvent was removed, and the crude oil was purified via flash chromatography to give a bright yellow-orange solid. This solid was triturated with diethyl ether to give 160 mg (0.44 mmol, 40% yield) of anhydride **31** (benzothienyl[4,5-*a*]benzothienyl[6,7-*a*]isobenzofuran-1,3-dione) as a bright-yellow solid: mp > 300 °C. <sup>1</sup>H NMR (DMSO-*d*<sub>6</sub>) δ: 9.54 (dd, *J* = 5.2 Hz, *J* = 2.5 Hz, 2H), 8.34 (dd, *J* = 4.0 Hz, *J* = 3.3 Hz, 2H), 7.73 (m, 4H). (b) **31** (75 mg, 0.2 mmol) in DMF (3 mL) was added to 1,1,1,3,3,3-hexamethyldisilazane (4.4 mL, 20.8 mmol), followed by 30 μL (1 mmol) of methanol. The suspension became clear after approximately 15 min. TLC after 1 h showed nearly complete consumption of the starting material. The reaction was allowed to stir overnight for a total reaction time of 18 h. Solvent was removed to give 65 mg (0.18 mmol, 80% yield) of **28** as a yellow solid: mp > 300 °C. <sup>1</sup>H NMR (DMSO-*d*<sub>6</sub>) δ: 9.8 (dd, *J* = 5.0 Hz, *J* = 4.1 Hz, 2H), 8.25 (dd, *J* = 4.9 Hz, *J* = 4.1 Hz, 2H), 7.70 (m, 4H); MS *m/z*: 360 (M + 1).

**Benzothieno[2,3-*c*]benzothieno[2,3-*e*]isoindol-1-one (32).** To a 10 mL ethanol suspension of Zn amalgam (3 equiv prepared as described for **26**) was added 68 mg (0.18 mmol) of **28** as a solution in 10 mL of acetic acid. Concentrated HCl (5 mL) was added, and the reaction was held at reflux overnight. The reaction, which became clear and tan in color, was cooled and decanted off of the mercury layer. After the solvent was removed, the mixture was diluted with ethyl acetate (50 mL) and washed with saturated NaHCO<sub>3</sub> (2 × 25 mL). The organic layer was dried over MgSO<sub>4</sub>, filtered, and the solvent was removed at reduced pressure. The crude reaction mixture was purified by silica gel column chromatography (95:5 CH<sub>2</sub>Cl<sub>2</sub>/MeOH) to give 65 mg (0.18 mmol, 100% yield) of **32** as a tan solid, mp 225–226 °C. <sup>1</sup>H NMR (DMSO-*d*<sub>6</sub>) δ: 10.17 (dd, *J* = 6.4 Hz, *J* = 2.7 Hz, 1H), 8.22 (s, 1H), 8.21 (dd, *J* = 4.1 Hz, *J* = 3.7 Hz, 2H), 8.11 (dd, *J* = 6.5 Hz, *J* = 2.2 Hz, 1H), 7.63 (t, *J* = 3.7 Hz, 2H), 7.55 (t, *J* = 3.7 Hz, 2H), 5.19 (s, 2H). MS *m/z*: 346 (M + 1).

**2-(2'-Indenyl)benzothiophene (34).** To a two-necked round-bottomed flask fitted with a reflux condenser was added 2-bromoindene<sup>18</sup> (2 g, 13.3 mmol), 2-(tri-*n*-butyltin)benzothiophene (5.1

g, 11.9 mmol), and 50 mL of toluene. To this mixture was added bis(triphenylphosphine) palladium(II) dichloride (1 g, 1.5 mmol) and BHT (5 mg). The reaction was held at reflux for 16 h. After cooling, the solvent was removed at reduced pressure, and the residue was dissolved in DMF/THF and filtered through celite. The solvent was removed, and the solid was triturated with hexanes to give 1.4 g (5.6 mmol, 47% yield) of **34** as an orange solid: mp 260–265 °C. <sup>1</sup>H NMR (DMSO-*d*<sub>6</sub>) δ: 7.82 (m, 4H), 7.61 (s, 1H), 7.35 (m, 5H), 3.97 (s, 2H).

**3,4-Carboethoxyindenyl[1,2-*a*]dibenzothiophene (35).** In a sealable glass tube was placed **33** (480 mg, 3.95 mmol), diethyl acetylenedicarboxylate (3.2 mL, 19 mmol), and BHT (10 mg). The reaction vessel was sealed under N<sub>2</sub> and held at 190 °C. The reaction was allowed to proceed for 24 h. After allowing the vessel to cool, the contents were transferred to a round-bottomed flask using CHCl<sub>3</sub>, and solvent was removed. The crude material was passed through a silica column, and the top fractions were collected. This solid was taken up in diethyl ether and filtered, giving 538 mg (1.29 mmol, 23%) of **35** as a pale-orange solid, mp 186 °C. <sup>1</sup>H NMR (DMSO-*d*<sub>6</sub>) δ: 8.15 (d, *J* = 7.4 Hz, 1H), 7.95 (d, *J* = 7.4 Hz, 1H), 7.71 (m, 2H), 7.56 (m, 2H), 7.41 (m, 2H), 4.50 (q, *J* = 7.0 Hz, 4H), 4.22 (s, 2H), 1.33 (t, *J* = 7.0 Hz, 6H).

**Indenyl[2,3-*c*]benzothienyl[2,3-*e*]isoindol-1,3-dione (33).** (a) A round-bottomed flask was charged with **35** (250 mg, 0.6 mmol) and pyridine (10 mL). To this mixture was added solid lithium iodide trihydrate (677 mg, 3.6 mmol). The reaction was held at 115 °C, followed by TLC. More LiI was added as time progressed. A total of 5 equiv of LiI was added over a reaction time of 36 h, at which time the starting material was totally consumed. The reaction mixture was cooled to room temperature and poured over cold (0 °C) aqueous HCl. The mixture was filtered and washed with water. The resultant solid was dried under vacuum. The above crude solid was then placed in a round-bottomed flask, and 50 mL of acetic anhydride was added. The reaction mixture was then held at reflux. After 4 h at reflux, the reaction was complete by TLC (new spot at *R*<sub>f</sub> 0.6 in 1:1 EtOAc/hexanes). The solvent was removed, and the crude oil was purified via flash chromatography to give a bright yellow-orange solid. This solid was triturated with diethyl ether to give anhydride **36** (indenyl[4,5-*a*]benzothienyl[6,7-*a*]isobenzofuran-1,3-dione) (160 mg, 0.44 mmol, 40% yield) as a bright yellow solid, mp > 300 °C. <sup>1</sup>H NMR (DMSO *d*<sub>6</sub>) δ: 9.65 (d, *J* = 7.2 Hz, 1H), 8.76 (d, *J* = 7.6 Hz, 1H), 8.15 (s, *J* = 7.4 Hz, 1H), 7.78–7.38 (m, 5H), 4.97 (s, 2H). (b) Anhydride **36** (120 mg, 0.35 mmol) was dissolved in 3 mL of DMF. To this mixture was added 1,1,1,3,3,3-hexamethyldisilazane (7.4 mL, 35 mmol) followed by methanol (50 μL, 1 mmol). The suspension became clear after approximately 15 min. TLC after 1 h showed nearly complete consumption of the starting material. The reaction was allowed to stir overnight for a total reaction time of 18 h. Solvent was removed to give 35 mg (0.18 mmol, 30% yield) of **33** as an orange solid, mp > 280 °C. <sup>1</sup>H NMR (DMSO-*d*<sub>6</sub>) δ: 12.72 (s, 1H), 9.84 (d, *J* = 8.3 Hz, 1H), 8.14 (d, *J* = 6.4 Hz, 1H), 8.07 (d, *J* = 7.5 Hz, 1H), 7.82–7.28 (m, 5H), 5.03 (s, 2H), MS *m/z*: 342 (M + H).

**Indenyl[2,3-*c*]benzothienyl[2,3-*e*]isoindol-1 (37) and 3-one (38).** A 2 mL ethanol suspension of Zn amalgam (3 eq prepared as described for **26**) was added to 10 mg (0.3 mmol) of **30** as a solution in 10 mL acetic acid. The reaction was held at reflux after the addition of 1 mL of concentrated HCl. After 3h at reflux, the reaction became clear and slightly tan. The reaction was cooled and decanted off of the mercury layer. After most of the solvent was removed, the mixture was diluted with ethyl acetate and washed two times with saturated NaHCO<sub>3</sub>. The organic layer was dried over MgSO<sub>4</sub>, was filtered, and solvent was removed to give the compound as a mixture of isomers as a tan solid. HPLC separation produced **37** and **38**.

**37:** mp > 280 °C. <sup>1</sup>H NMR (DMSO-*d*<sub>6</sub>) δ: 10.15 (d, *J* = 5 Hz, 1H), 9.04 (s, 1H), 8.11 (d, *J* = 5 Hz, 1H), 7.83 (d, *J* = 7.2 Hz, 1H), 7.74 (d, *J* = 7 Hz, 1H), 7.74–7.59 (m, 4H), 5.08 (s, 2H), 4.28 (s, 2H). MS *m/z*: 328 (M + 1).

38: mp > 280 °C. <sup>1</sup>H NMR (DMSO-*d*<sub>6</sub>) δ: 9.38 (d, *J* = 7.3 Hz, 1H), 8.94 (s, 1H), 8.14–8.16 (m, 2H), 7.60–7.69 (m, 3H), 7.74–7.46 (m, 2H), 5.06 (s, 2H), 4.20 (s, 2H). MS *m/z*: 328 (M + 1).

**Mixed-Lineage Kinase Assays.** The MLK1, MLK2, and MLK3 assays were performed using the Millipore multiscreen trichloroacetic acid (TCA) “in-plate” format as described previously.<sup>8</sup> Each 50 μL assay mixture contained 20 mM Hepes, pH 7.2, 5 mM EGTA, 15 mM MgCl<sub>2</sub>, 1 mM DTT, 25 mM β-glycerophosphate, the *K<sub>m</sub>* level of ATP (60 μM for MLK1 or 100 μM for MLK2 and MLK3), 0.25 μCi [<sup>γ</sup>-<sup>32</sup>P]ATP, 0.1% BSA, 2% DMSO, and 500 μg/mL myelin basic protein. The reaction was initiated by adding purified recombinant kinases (50, 150, and 100 ng of GST-MLK1<sub>KD</sub>, GST-MLK2<sub>KD/LZ</sub>, and GST-MLK3<sub>KD</sub>, respectively). The samples were incubated for 15 min at 37 °C. The reaction was stopped by adding ice-cold 50% TCA, and the proteins were allowed to precipitate for 30 min at 4 °C. The plates were then washed with ice-cold 25% TCA. A supermix scintillation cocktail was added, and the plates were allowed to equilibrate for 1 to 2 h prior to counting using the Wallac MicroBeta 1450 PLUS scintillation counter. Inhibition curves for the compounds were generated by plotting the percent control activity versus the log of the concentration of the compound. IC<sub>50</sub> values were calculated by nonlinear regression using the sigmoidal dose–response (variable slope) equation in GraphPad Prism as follows:  $y = \text{bottom} + (\text{top} - \text{bottom}) / (1 + 10^{(\log IC_{50} - x) * \text{HillSlope}})$ , where *y* is the percent kinase activity at a given concentration of compound, *x* is the logarithm of the concentration of the compound, bottom is the percent of control kinase activity at the highest compound concentration tested, and top is the percent of control kinase activity at the lowest compound concentration examined. The values for bottom and top were fixed at 0 and 100, respectively. The IC<sub>50</sub> values were reported as the averages of duplicates that agree to within 20%.

**Other Kinase Assays.** Inhibition assays for recombinant receptor tyrosine kinases (EGFR, FGFR1, βIRK, PDGFRβ, TIE2, TrkA, and VEGFR2) and serine/threonine kinases (CDK1, CDK2, DLK, JNK1, p38α, and PKC) were performed as described previously.<sup>27–29</sup>

**Acknowledgment.** We acknowledge the scientific contributions of and helpful discussions with Mark Ator, Ed Bacon, Jim Diebold, Marcie Glicksman, Jean Husten, Sherri Meyer, Chung Ho Park, Dave Rotella, Mary Savage, and Shi Yang.

**Supporting Information Available:** Elemental analysis of compounds. This material is available free of charge via the Internet at <http://pubs.acs.org>.

## References

- (a) Hirsch, E. C.; Hunot, S.; Faucheux, B.; Agid, Y.; Mizuno, Y.; Mochizuki, H.; Tatton, W. G.; Tatton, N.; Olanow, W. C. Dopaminergic neurons degenerate by apoptosis in Parkinson's disease. *Mov. Disord.* **1999**, *14*, 383–385. (b) Hartman, A.; Hunot, S.; Michel, P. P.; Muriel, M. P.; Vyas, S.; Faucheux, B.; Mouatt-Prigent, A.; Turmel, H.; Srinivasan, A.; Ruberg, M.; Evan, G. I.; Agid, Y.; Hirsch, E. C. Caspase-3: A vulnerability factor and final effector in apoptotic death of dopaminergic neurons in Parkinson's disease. *Proc. Natl. Acad. Sci. U.S.A.* **2000**, *97*, 2875–2880. (c) Anderson, A. J.; Su, J. H.; Cotman, C. W. DNA damage and apoptosis in Alzheimer's disease: colocalization with c-Jun immunoreactivity, relationship to brain area, and effect of postmortem delay. *J. Neurosci.* **1996**, *16*, 1710–1719.
- (a) Bozyczko-Coyne D.; Saporito, M. S.; Hudkins, R. L. Targeting the JNK pathway for therapeutic benefit in CNS disease. *Curr. Drug Targets: CNS Neurol. Disord.* **2002**, *1*, 31–49. (b) Bogoyevitch, M. A.; Boehm, I.; Oakley, A.; Ketterman, A. J.; Barr, R. K. Targeting the JNK MAPK cascade for inhibition: basic science and therapeutic potential. *Biochim. Biophys. Acta* **2004**, *1697*, 89–101. (c) Manning, A. M.; Davis, R. J. Targeting JNK for therapeutic benefit: from junk to gold? *Nat. Rev. Drug Discovery* **2003**, *2*, 554–564. (d) Harper, S. J.; LoGrasso, P. Signaling for survival and death in neurons. The role of stress-activated kinases, JNK and p38. *Cell. Signalling* **2001**, *13*, 299–310. (e) Mielke, K.; Herdegen, T. JNK and p28 stress kinases – degenerative effectors of signal-transduction-cascades in the nervous system. *Prog. Neurobiol.* **2000**, *61*, 45–60.
- (a) Gupta, S.; Barrett, T.; Whitmarsh, A. J.; Cavanagh, J.; Sluss, H. K.; Derijard, B.; Davis, R. J. Selective interaction of JNK protein kinase isoforms with transcription factors. *EMBO J.* **1996**, *15*, 2760–2770. (b) Kallunki, T.; Su, B.; Tsigelny, I. Sluss, H. K.; Derijard, B.; Moore, G.; Davis, R.; Karin, M. JNK2 contains a specificity-determining region responsible for efficient c-Jun binding and phosphorylation. *Genes Dev.* **1994**, *8*, 2996–3007. (c) Kallunki, T.; Deng, T.; Hibi, M.; Karin, M. c-Jun can recruit JNK to phosphorylate dimerization partners via specific docking interactions. *Cell* **1996**, *87*, 1–20.
- (a) Maroney, A. C.; Saporito, M. A.; Hudkins, R. L. Mixed lineage kinase family, potential targets for preventing neurodegeneration. *Curr. Med. Chem: Cent. Nerv. Syst. Agents* **2002**, *2*, 143–155. (b) Wang, L. H.; Besirli, C. G.; Johnson, E., Jr. Mixed lineage kinases: A target for the prevention of neurodegeneration. *Annu. Rev. Pharmacol. Toxicol.* **2004**, *44*, 451–474. (c) Gallo, K. A.; Johnson, G. L. Mixed-lineage kinase control of JNK and p38 MAPK pathways. *Nat. Rev. Mol. Biol.* **2002**, *3*, 663–672.
- (a) Xu, Z.; Maroney, A. C.; Dobrzanski, P.; Kukekov, N. V.; Greene, L. A. The MLK family mediates c-Jun N-terminal kinase activation in neuronal apoptosis. *Mol. Cell Biol.* **2001**, *21*, 4713–4724. (b) Mota, M.; Reeder, M.; Chernoff, J.; Bazenot, C. E. Evidence for a role of mixed lineage kinases in neuronal apoptosis. *J. Neurosci.* **2001**, *21*, 4949–4957.
- (a) Murakata, C.; Kaneko, M.; Gessner, G.; Angeles, T. S.; Ator, M. A.; O'Kane, T. M.; McKenna, B. A. W.; Thomas, B. A.; Mathiasen, J. R.; Saporito, M. S.; Bozyczko-Coyne, D.; Hudkins, R. L. Mixed Lineage kinase activity of indolocarbazole analogs. *Bioorg. Med. Chem. Lett.* **2002**, *12*, 147–150.
- (a) Saporito, M. A.; Hudkins, R. L.; Maroney, A. C. Discovery of CEP-1347/KT-7515: An inhibitor of the cJun N-terminal kinase pathway for the treatment of neurodegenerative diseases. *Prog. Med. Chem.* **2002**, *40*, 23–62. (b) Glicksman, M. A.; Chiu, A. Y.; Dionne, C. A.; Kaneko, M.; Murakata, C.; Oppenheim, R. W.; Prevette, D.; Sengelaub, D. R.; Vaught, J. L.; Neff, N. T. CEP-1347/KT7515 prevents motor neuronal programmed cell death and injury-induced dedifferentiation in vivo. *J. Neurobiol.* **1998**, *35*, 361–370. (c) Borasio, G. D.; Hostmann, S.; Anneser, J. M. H.; Neff, N. T.; Glicksman, M. A. CEP-1347/KT7515, a JNK pathway inhibitor, supports the in vitro survival of chick embryonic neurons. *NeuroReport* **1998**, *9*, 1435–1439.
- (a) Maroney, A. C.; Finn, J. P.; Connors, T. J.; Durkin, J. T.; Angeles, T.; Gessner, G.; Xu, Z.; Meyer, S. L.; Savage, M. J.; Greene, L. A.; Scott, R. W.; Vaught, J. L. CEP-1347 (KT-7515), a semisynthetic inhibitor of the mixed lineage kinase family. *J. Biol. Chem.* **2001**, *276*, 25302–25308.
- (a) Saporito, M. S.; Brown, E. M.; Miller, M. S.; Carswell, S. CEP-1347/KT7515, an inhibitor of c-Jun N-terminal kinase activation, attenuates the 1-methyl-4-phenyl tetrahydropyridine-mediated loss of nigrostriatal dopaminergic neurons in vivo. *J. Pharmacol. Exp. Ther.* **1999**, *288*, 421–427. (b) Saporito, M. S.; Thomas, B. A.; Scott, R. W. MPTP activates c-jun NH<sub>2</sub>-terminal kinase (JNK) and its upstream regulator kinase MKK4 in nigrostriatal neurons in vivo. *J. Neurochem.* **2000**, *75*, 1200–1208.
- (a) Kaneko, M.; Saito, Y.; Saito, H.; Matsumoto, T.; Matsuda, Y.; Vaught, J. L.; Dionne, C. A.; Angeles, T. S.; Glicksman, M. A.; Neff, N. T.; Rotella, D. P.; Kauer, J. C.; Mallamo, J. P.; Hudkins, R. L.; Murakata, C. Neurotrophic 3,9-bis[(alkylthiomethyl)]- and -[bis-(alkoxymethyl)]-K-252a Derivatives. *J. Med. Chem.* **1997**, *40*, 1863–1869.
- (a) Kase, H.; Iwahashi, K.; Matsuda, Y. K-252a, a potent inhibitor of protein kinase C from microbial origin. *J. Antibiot.* **1986**, *39*, 1059–1065.
- (a) Nakanishi, S.; Matsuda, K.; Iwahashi, K.; Kase, H. K-252b, c and d, potent inhibitors of protein kinase C from microbial origin. *J. Antibiot.* **1986**, *39*, 1066–1071.
- (a) Schiering, N.; Knapp, S.; Marconi, M.; Flocco, M. M.; Cui, J.; Perego, R.; Rusconi, L.; Cristiani, C. Crystal structure of the tyrosine kinase domain of the hepatocyte growth factor receptor c-Met and its complex with the microbial alkaloid K-252a. *Proc. Natl. Acad. Sci. U.S.A.* **2003**, *22*, 12654–12659.
- (a) Hudkins, R. L.; Park, C-H. Synthesis of indeno[2, 1-a]pyrrolo[3,4-c]carbazole lactam regioisomers using ethyl cis-β-cyanoacrylate as a dienophile and lactam precursor. *J. Heterocycl. Chem.* **2003**, *40*, 135–142.
- (a) Hudkins, R. L.; Johnson, N. W. Synthesis of benzo[b]thieno- and benzo[b]furan[2,3-a]pyrrolo[3,4-c]carbazole-5-, -7- and -5,7-dione. *J. Heterocycl. Chem.* **2001**, *38*, 591–595.
- (a) Baierweck, P.; Simmross, U.; Muellen, K. Biindenyls, biindenylides and diindenyl-fused heterocycles from oxidative coupling of 1- and 2-indanone. *Chem. Ber.* **1988**, *121*, 2195–2200.

- (17) (a) Hudkins, R. L.; Johnson, N. W. Fused Isoindolones as Inhibitors, of PKC. U.S. Patent 5,705,511, 1997. (b) Hudkins, R. L.; Johnson, N. W. Fused Isoindolones. U.S. Patent 5,808,060, 1998.
- (18) Lindley, W. A.; MacDowell, D. W. H. Keto-enol tautomerism in the thiophene analogs of naphthacen-5-one. *J. Org. Chem.* **1982**, *47*, 705–709.
- (19) Rotella, D. P.; Glicksman, M. A.; Prantner, J. E.; Neff, N. T.; Hudkins, R. L. The effect of pyrrolo[3,4-c]carbazole derivatives on spinal cord ChAT activity. *Bioorg. Med. Chem. Lett.* **1995**, *5*, 1167–1170.
- (20) Ator, M. A.; Chatterjee, S.; Bihovski, R.; Dunn; Hudkins, R. L. Multicyclic PARP and kinase inhibitors. WO0185686, 2001.
- (21) Hudkins, R. L.; Fused Isoindolones. U.S. Patent 6,399,780, 2005.
- (22) Gingrich, D. L.; Yang, S. X.; Gessner, G. W.; Angeles, T. S.; Hudkins, R. L. Synthesis, modeling and in vitro activity of 3'-(S)-*epi*-K-252a analogues. Elucidating the stereochemical requirements of the 3'-sugar alcohol on trkA tyrosine kinase activity. *J. Med. Chem.* **2005**, *48*, 3776–3783.
- (23) Ruggeri, B. A.; Miknyoczki, S. J.; Singh, J.; Hudkins, R. L.; The role of neurotrophin-trk interactions in oncology: The antitumor efficacy of potent and selective trk tyrosine kinase inhibitors on preclinical tumor models. *Curr. Med. Chem.* **1999**, *6*, 845–857.
- (24) (a) Glicksman, M. A.; Prantner, J. E.; Meyer, S. L.; Forbes, M. E.; Dasgupta, M.; Lewis, M. E.; Neff, N. T. K-252a and staurosporine promote choline acetyltransferase activity in rat spinal cord culture. *J. Neurochem.* **1993**, *61*, 210–221. (b) Glicksman, M. A.; Forbes, M. E.; Prantner, J. E.; Neff, N. T. K-252a promotes survival and choline acetyltransferase activity in striatal and basal forebrain neuronal cultures. *J. Neurochem.* **1995**, *64*, 1502–1512.
- (25) Phelps, P. E.; Barber, R. P.; Vaughn, J. E. Generation patterns of four groups of cholinergic neurons in rat cervical spinal cord: a combined tritiated thymidine autoradiographic and choline acetyltransferase immunocytochemical study. *J. Comp. Neurol.* **1988**, *273*, 459–472.
- (26) (a) Hartikka, K. J.; Hefti, F. Development of septal cholinergic neurons in culture: plating density and glial cells modulate effects of NGF on survival, fiber growth and expression of transmitter-specific enzymes. *J. Neurosci.* **1988**, *8*, 2967–2985. (b) Lewis, M. E.; Neff, N. T.; Contreras, P. C.; Stong, D. B.; Oppenheim, R. W.; Grebow, P. E.; Vaught, J. L. Insulin-like growth factor-I: potential for treatment of motor neuronal disorders. *Exp. Neurol.* **1993**, *124*, 73–88. (c) Neff, N. T.; Prevette, D.; Houenou, L. J.; Lewis, M. E.; Glicksman, M. A.; Yin, Q. W.; Oppenheim, R. W. Insulin-like growth factors: Putative muscle derived trophic agents that promote motoneuron survival. *J. Neurobiol.* **1993**, *24*, 1578–1588.
- (27) Gingrich, D. E.; Reddy, D. R.; Iqbal, M. A.; Singh, J.; Aimone, L. D.; Angeles, T. S.; Albom, M.; Yang, S.; Meyer, S.; Robinson, C.; Ruggeri, B. A.; Dionne, C. A.; Vaught, J. L.; Mallamo, J. P.; Hudkins, R. L. A new class of potent VEGF receptor tyrosine kinase inhibitors: Structure-activity relationships for a series of 9-alkoxymethyl-12-(3-hydroxypropyl)indeno[2,1-a]pyrrolo[3,4-c]carbazole-5-ones and the identification of CEP-5214 and its dimethylglycine ester prodrug clinical candidate CEP-7055. *J. Med. Chem.* **2003**, *46*, 5375–5388.
- (28) Angeles, T. S.; Steffler, C.; Bartlett, B. A.; Hudkins, R. L.; Stephens, R. M.; Kaplan, D. R.; Dionne, C. A. Enzyme linked immunosorbant assay for TrkA tyrosine kinase activity. *Anal. Biochem.* **1996**, *236*, 49–55.
- (29) Ruggeri, B.; Singh, J.; Gingrich, D.; Angeles, T.; Albom, M.; Chang, H.; Robinson, C.; Hunter, K.; Dobrzanski, P.; Jones-Bolin, S.; Aimone, L.; Klein-Szanto, A.; Herbert, J.-M.; Bono, F.; Casellas, P.; Bourie, B.; Pili, R.; Isaacs, J.; Ator, M.; Hudkins, R.; Dionne, C.; Mallamo, J.; Vaught, J. CEP-7055: A novel, orally-active pan inhibitor of vascular endothelial growth factor receptor tyrosine kinases with potent anti-angiogenic activity and anti-tumor efficacy in pre-clinical models. *Cancer Res.* **2003**, *63*, 5978–5991.

JM051074U